




NOTE

Georgios I. Dadoulis · George D. Manolis 

A comparative study on the effectiveness of a moving versus a fixed passive damper in beam vibration mitigation

Received: 29 March 2024 / Revised: 17 July 2024 / Accepted: 21 July 2024
© The Author(s), under exclusive licence to Springer-Verlag GmbH Austria, part of Springer Nature 2024

Abstract This work compares the effect that two categories of passive dampers have on the vibratory motion of a bridge modeled as simply supported uniform beam, namely the fixed versus the moving tuned mass damper (TMD). Assuming that the suspension system of the moving vehicle performs like a TMD, its effect on the vibratory motion at points on the beam is studied by juxtaposing it with the performance of the same system placed at a specific location on the bridge span. In both cases, the vehicle suspension is modeled as a single degree-of freedom (SDOF) system with a mass, a stiffness and a damping element. Specifically, we first examine the eigenproblem of this combined structural system comprising the bridge, the moving mass and the TMD, to compute spectrograms that show the time–frequency evolution of the eigenfrequencies for both fixed and moving TMD cases. Subsequently, we examine vibrations at a point close to center span of the beam and produce energy measures to contrast fixed versus moving TMD effectiveness, which changes over time thus making it impossible to produce a concrete measure.

1 Introduction

The use of tuned mass dampers (TMD) as vibration absorption devices within a structural system has a long history dating to over a hundred years [1]. TMD's are classified as passive devices in the sense that they are activated when the primary system they are attached to starts to vibrate [2]. As such, they require no external power source to function as their performance simply depends on a combination of lumped mass, spring and dashpot components. The choice of these components is usually based on optimizing their performance for harmonic loads, which implies that they may not be as effective for other categories of loads such as impact, random, etc. [3]. In this case, they can be classified as sub-optimal TMD. Another parameter of TMD design and performance is their actual placement, which means that the designer has to decide on both the number and the location where they best perform.

As the literature on TMD's is vast, we will briefly survey some recent work done in reference to the subject of vehicles traversing a bridge. In particular, bridge vibrations are a crucial issue in structural health monitoring (SHM), since they are one of the main reasons behind bridge performance deterioration, other reasons being corrosion, temperature variation, support movement, etc. [4]. In particular, two aspects of this problem have attracted attention: (a) The role that the suspension system of the moving vehicle plays in ameliorating not only its own vibrations, but those induced to the bridge; (b) the change in the dynamic characteristics of the bridge (natural frequencies and associated modes) when the mass of the moving vehicle is roughly comparable

G. I. Dadoulis · G. D. Manolis (✉)
Laboratory for Experimental Strength of Materials and Structures, Department of Civil Engineering,
Aristotle University, 54124 Thessaloniki, Greece
e-mail: gdm@civil.auth.gr

G. I. Dadoulis
e-mail: dadoulis@civil.auth.gr

to that of the bridge. References [5–14] address these issues, encompassing numerical-analytical models, experimental results, field measurements and also examining a variety of forcing functions.

As mentioned, bridge vibration mitigation through tuning of the vehicle suspension parameters is a topic of current interest. Earlier work [5] investigated the dynamic response of short-span bridges produced by the passage of heavy vehicles with two different types of suspensions. The solution methodology combined the modal shapes of the bridge with the dynamic wheel loads in a time-convolution integral, while the surface profile of the bridge was also taken into account. A parametric study followed to ascertain which type of suspension system is the most effective for vibration mitigation. One of the earliest experimental evaluations aimed at measuring the time evolution of bridge modal properties during the passage of a single vehicle was reported in [6]. Specifically, two bridges were instrumented for both traversing and parked trucks and the measurements were processed by an output-only technique using the continuous wavelet transformation. Shifts in the eigenproperties of the bridges were indeed detected, and a simplified numerical model was developed to quantify them. Stochasticity was introduced as a means of capturing uncertainties in vehicles traversing a bridge [7]. Specifically, a Gaussian distribution of the vehicle parameters was assumed, followed by Monte Carlo simulations that gave the statistical measures of the dynamic response of the bridge. However, no mention was made regarding the influence of the moving loads on the bridge eigenproperties.

The question of instantaneous frequencies of bridges under moving vehicles is discussed in [8], where a theoretical framework was presented for both structure and vehicle frequency variations. An analytical solution was based on eigenvalue extraction for the coupled bridge-vehicle dynamical system, which was used to identify the dominant factors behind this problem and yielded as special cases the moving force and the moving mass. Mitigation of the dynamic response of a bridge by tuning the vehicle suspension parameters was recently studied in [9] by considering a quarter-car model with semi-active suspension. Transmissibility functions were derived for this time-dependent system, which showed that the frequency response of the bridge depends primarily on the vehicle-bridge frequency and damping ratios. However, it is difficult to define a transmissibility function for a time-dependent dynamic system. Next, the change of a bridge's natural frequencies with respect to the position of the traversing vehicle was studied in [10] by conducting measurements on a scaled model of a bridge. It was empirically shown that both direct (sensor on the bridge) and indirect (sensor on the vehicle) records showed that the bridge frequency shift depended primarily on the bridge-to-vehicle frequency ratio. Next, a single-axle test vehicle, which was used in scanning the roughness of bridge surfaces [11], was further examined from the viewpoint of dynamic interaction with the bridge that may adversely affect data quality. A frequency-free vehicle was proposed as a means for avoiding this interaction phenomenon by assuring that its natural frequency falls far beyond that of the bridge. Another alternative proposed was the parked state of the vehicle. Laboratory tests were also conducted with two-axle vehicles under ambient vibrations, as well as benchmark test for a real bridge. Finally, in reference to railroad bridges traverse by massive and directionally moving cars, the temporal variation of the fundamental frequencies of both systems was studied in [12]. Given the difficulty in developing analytical solutions, a time–frequency analysis was used with the modified Stockwell transform for optimizing the spatial–temporal energy distribution of the combined dynamic system. Following this development for a single moving vehicle, a machine learning technique was subsequently employed to extract multi-vehicle interaction frequencies, which were further validated with data from scaled laboratory experiments.

The difficulty presented in damage detection techniques based on bridge resonances during the passage of traffic was studied in [13], given the fact that bridge-vehicle interaction results in the development of a coupled dynamic system. A vehicle-induced delta frequency function was introduced to account for changes in the bridge's time-varying resonance, followed by a damage-induced delta frequency function to account for additional changes caused by damage in the bridge. This problem was studied for railway bridges, focusing on the difference between single and dual suspension train systems. Finally, the effect of the placement of a fixed TMD in a vehicle-bridge coupled system was studied in [14], where the mechanics of bridge-vehicle interaction were accounted for. The bridge response in the presence of a TMD to both a moving as well as a parked vehicle was examined when the source of vibration is earthquake-induced ground motions causing vertical motions in the bridge.

In what follows, an experimental study of a model bridge span that was tested for a moving heavy mass [15] was re-visited by conducting a numerical study based on the underlying mathematical model with an added TMD. This TMD was first placed at a fixed location at center span of the bridge and subsequently attached under the heavy moving mass. Results showed that energy dissipation by these TMD systems is time-dependent, which makes it difficult to establish superior performance by either one, when the design criterion is vibration minimization at a specific point on the bridge.

2 Statement of the problem

A heavy mass moving across the span of a bridge is often linked to a suspension system comprising a spring plus a damper. It turns out that this configuration is equivalent to a tuned mass damper (TMD) through which a time-dependent load is transmitted to the span. We note in passing that if the mass is heavy as compared to the weight of the span itself, the eigenvalue problem becomes time-dependent since the mass of the combined system changes during the passage time. From another viewpoint, it is possible to attach a single degree-of-freedom (SDOF) secondary system to a fixed location on the bridge, which is the primary structural system, for the purpose of vibration suppression. Thus, an interesting problem arises as to which configuration is most effective, assuming that it is possible to choose either one. The problem is illustrated in Fig. 1 for a simply supported beam span of length L and flexural stiffness EI . Furthermore, the heavy moving mass is denoted as M , the mass of the attached passive damper as m , while k , c are spring and damper elements in the TMD, respectively. Finally, $w(x, t)$ is the beam's transverse displacement, $u_r(t)$ is the relative displacement between a point mass and its attachment where the internal force f_C develops, while $r(x)$ is the roughness of the upper surface of the beam.

3 Equations of motion

The mechanical representation of the combined structural system consists of the primary structure (bridge) that is modeled as a continuous beam to which a secondary system (TMD) modeled as an SDOF is attached. At first, the transverse displacement of the beam is expressed in terms of its eigenfunctions and the corresponding generalized coordinates as $w(x, t) = \Phi_i(x)q_i(t)$, $i = 1, 2, \dots$. Next, in Table 1 we define the position vectors of the structural system with respect to its static equilibrium configuration.

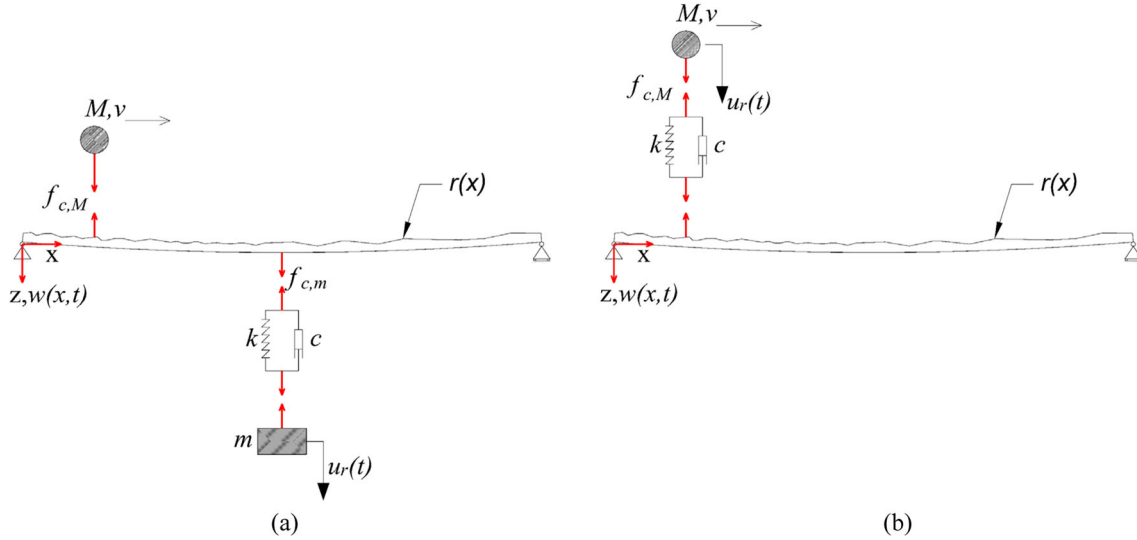


Fig. 1 Free body diagram of a simply supported beam traversed by a heavy mass: **a** TMD attached at center span and **b** the moving mass acting as a TMD

Table 1 Position vectors \vec{r} defined for the beam, the moving mass M and the attached mass m

TMD attached at $x = L_1 = L/2$	Moving mass M acting as the TMD
$\vec{r}_{beam} = (0, 0, \Phi_i(x)q_i(t))$	$\vec{r}_{beam} = (0, 0, \Phi_i(x)q_i(t))$
$\vec{r}_m = (0, 0, \Phi_i(L_1)q_i(t) + u_r(t))$	$\vec{r}_m = (0, 0, \Phi_i(L_1)q_i(t) + u_r(t))$
$\vec{r}_M = (vt, 0, \Phi_i(vt)q_i(t) + r(x(t)))$	$\vec{r}_M = (vt, 0, \Phi_i(vt)q_i(t) + u_r(t) + r(x(t)))$

An energy approach for case (a), the attached TMD, defines the potential energy U and the kinetic energy T of the combined system as follows:

$$U(\mathbf{q}) = \frac{1}{2}ku_r^2 + \frac{1}{2}\omega_i^2q_i^2 - Mg(\Phi_i(vt)q_i(t) + r(x(t))) \quad (1a)$$

$$T(\mathbf{q}) = \frac{1}{2}\dot{q}_i^2 + \frac{1}{2}m(\Phi_i(L_1)\dot{q}_i(t) + \dot{u}_r(t))^2 + \frac{1}{2}M\left(\Phi_i'(vt)vq_i(t) + \Phi_i(vt)\dot{q}_i(t) + r'(x(t))v\right)^2 + \frac{1}{2}Mv^2 \quad (1b)$$

For case (b) where the moving mass simultaneously behaves as a TMD, the potential and kinetic energies are now equal to

$$U(\mathbf{q}) = \frac{1}{2}ku_r^2 + \frac{1}{2}\omega_i^2q_i^2 - Mg(\Phi_i(vt)q_i(t) + r(x(t))) \quad (2a)$$

$$T(\mathbf{q}) = \frac{1}{2}\dot{q}_i^2 + \frac{1}{2}M\left(\Phi_i'(vt)vq_i(t) + \Phi_i(vt)\dot{q}_i(t) + \dot{u}_r(t) + r'(x(t))v\right)^2 + \frac{1}{2}Mv^2 \quad (2b)$$

Note the vector $\mathbf{q} = (q_i, u_r)$, $i = 1, 2$ and that the first two eigenfunctions of the beam are used in this representation.

Using the previously defined energy terms, Lagrange's equations for the combined system modeled by the first two eigenfunctions and the relative displacement are

$$\begin{aligned} \frac{d}{dt}\left(\frac{\partial T}{\partial \dot{q}_i}\right) - \frac{\partial T}{\partial q_i} + \frac{\partial U}{\partial q_i} + c_i^*\dot{q}_i &= 0, i = 1, 2 \\ \frac{d}{dt}\left(\frac{\partial T}{\partial \dot{u}_r}\right) - \frac{\partial T}{\partial u_r} + \frac{\partial U}{\partial u_r} + c^*\dot{u}_r &= 0 \end{aligned} \quad (3)$$

The RHS of the above equation is zero because of the absence of external forces and of non-conservative fields. After substitution of the energy terms in the above equations and following manipulations, a system of finite element method-like results for the generalized coordinate vector \mathbf{q} is as follows:

$$\mathbf{M}(t)\ddot{\mathbf{q}}(t) + \mathbf{C}(t)\dot{\mathbf{q}}(t) + \mathbf{K}(t)\mathbf{q}(t) = \mathbf{F}(t) \quad (4)$$

The terms appearing in Eq. (4) are listed below, with index $j = 1$ denoting the case where the TMD is attached at location $x = L/2 = L_1$, while index $j = 2$ denotes the heavy mass acting as a moving TMD. In both cases, ω_i , $i = 1, 2$ are the eigenfrequencies and ξ_i the corresponding modal damping ratios of the simply supported beam without the moving mass or the TMD, i.e., the primary system. It is noted that in the bibliography these equations appear in different forms, depending on whether the generalized coordinates are defined with respect to the static deflection of the combined structural system or not.

$$\begin{aligned} \mathbf{M}(t) &= \begin{bmatrix} 1 + M\Phi_1(vt)\Phi_1(vt) & M\Phi_1(vt)\Phi_2(vt) & 0 \\ M\Phi_2(vt)\Phi_1(vt) & 1 + M\Phi_2(vt)\Phi_2(vt) & 0 \\ 0 & 0 & 0 \end{bmatrix} + \mathbf{M}_{\text{TMD}}^j \\ \mathbf{C}(t) &= \begin{bmatrix} 2Mv\Phi_1(vt)\Phi_1'(vt) + 2\omega_1\xi_1 & 2Mv\Phi_1(vt)\Phi_2'(vt) & 0 \\ 2Mv\Phi_2(vt)\Phi_1'(vt) & 2Mv\Phi_2(vt)\Phi_2'(vt) + 2\omega_2\xi_2 & 0 \\ 0 & 0 & 0 \end{bmatrix} + \mathbf{C}_{\text{TMD}}^j \\ \mathbf{K}(t) &= \begin{bmatrix} Mv^2\Phi_1(vt)\Phi_1''(vt) + \omega_1^2 & Mv^2\Phi_1(vt)\Phi_2''(vt) & 0 \\ Mv^2\Phi_2(vt)\Phi_1''(vt) & Mv^2\Phi_2(vt)\Phi_2''(vt) + \omega_2^2 & 0 \\ 0 & 0 & 0 \end{bmatrix} + \mathbf{K}_{\text{TMD}}^j \\ \mathbf{F}(t) &= \begin{bmatrix} (Mg - Mv^2r''(x(t)))\Phi_1(vt) \\ (Mg - Mv^2r''(x(t)))\Phi_2(vt) \\ 0 \end{bmatrix} + \mathbf{F}_{\text{TMD}}^j \end{aligned} \quad (5)$$

$$\begin{aligned}
\mathbf{M}_{\text{TMD}}^{\text{j}=1} &= \begin{bmatrix} m\Phi_1(L_1)\Phi_1(L_1) & m\Phi_1(L_1)\Phi_2(L_1) & m\Phi_1(L_1) \\ m\Phi_2(L_1)\Phi_1(L_1) & m\Phi_2(L_1)\Phi_2(L_1) & m\Phi_2(L_1) \\ \Phi_1(L_1) & \Phi_2(L_1) & 1 \end{bmatrix}, \\
\mathbf{C}_{\text{TMD}}^{\text{j}=1} &= \begin{bmatrix} 0 & 0 & 0 \\ 0 & 0 & 0 \\ 0 & 0 & 2\omega\xi \end{bmatrix}, \quad \mathbf{K}_{\text{TMD}}^{\text{j}=1} = \begin{bmatrix} 0 & 0 & 0 \\ 0 & 0 & 0 \\ 0 & 0 & \omega^2 \end{bmatrix}, \quad \mathbf{F}_{\text{TMD}}^{\text{j}=1} = \begin{Bmatrix} 0 \\ 0 \\ 0 \end{Bmatrix}, \\
\mathbf{M}_{\text{TMD}}^{\text{j}=2} &= \begin{bmatrix} 0 & 0 & M\Phi_1(vt) \\ 0 & 0 & M\Phi_2(vt) \\ \Phi_1(vt) & \Phi_2(vt) & 1 \end{bmatrix}, \quad \mathbf{C}_{\text{TMD}}^{\text{j}=2} = \begin{bmatrix} 0 & 0 & 0 \\ 0 & 0 & 0 \\ 2v\Phi_1'(vt) & 2v\Phi_2'(vt) & 2\omega\xi \end{bmatrix}, \\
\mathbf{K}_{\text{TMD}}^{\text{j}=2} &= \begin{bmatrix} 0 & 0 & 0 \\ 0 & 0 & 0 \\ v^2\Phi_1''(vt) & v^2\Phi_2''(vt) & \omega^2 \end{bmatrix}, \quad \mathbf{F}_{\text{TMD}}^{\text{j}=2} = \begin{Bmatrix} 0 \\ 0 \\ -v^2 r''(x(t)) \end{Bmatrix}
\end{aligned} \tag{6}$$

4 Numerical solution

The above systems of second-order, matrix differential equations are solved by recasting it as a system of first-order differential equations of twice the size, i.e.,

$$\mathbf{A}(t)\dot{\mathbf{y}}(t) + \mathbf{B}(t)\mathbf{y}(t) = \mathbf{h}(t) \tag{7}$$

where

$$\mathbf{A}(t) = \begin{bmatrix} \mathbf{0} & \mathbf{M}(t) \\ \mathbf{M}(t) & \mathbf{C}(t) \end{bmatrix}, \quad \mathbf{B}(t) = \begin{bmatrix} -\mathbf{M}(t) & \mathbf{0} \\ \mathbf{0} & \mathbf{K}(t) \end{bmatrix}, \quad \mathbf{y}(t) = \begin{Bmatrix} \dot{q}_1 \\ \dot{q}_2 \\ \dot{u}_r \\ q_1 \\ q_2 \\ u_r \end{Bmatrix}, \quad \mathbf{h}(t) = \begin{Bmatrix} \mathbf{0} \\ \mathbf{F}(t) \end{Bmatrix}$$

The transient response is computed by discretizing the time axis in $n = 1, 2, \dots, N$ time steps Δt , where the total time of interest is $t_{\text{total}} = N\Delta t = L/v$. Thus, Eq. (7) is solved for $\dot{\mathbf{y}}(t)$ stepwise as:

$$\dot{\mathbf{y}}_n(n\Delta t) = (-\mathbf{A}_n^{-1}(n\Delta t)\mathbf{B}_n(n\Delta t))\mathbf{y}_n(n\Delta t) + \mathbf{A}_n^{-1}(n\Delta t)\mathbf{h}_n(n\Delta t) \tag{8}$$

It is assumed that all matrices remain constant over the duration of a time step. Equation (7) can be solved for each time step by either the fundamental matrix approach [17] or by use of the Laplace transform [15]. In here, the former approach was used that requires the solution of an eigenvalue problem during each time step Δt for extraction of the time-dependent eigenfunctions and their corresponding eigenfrequencies, as derived from system matrix:

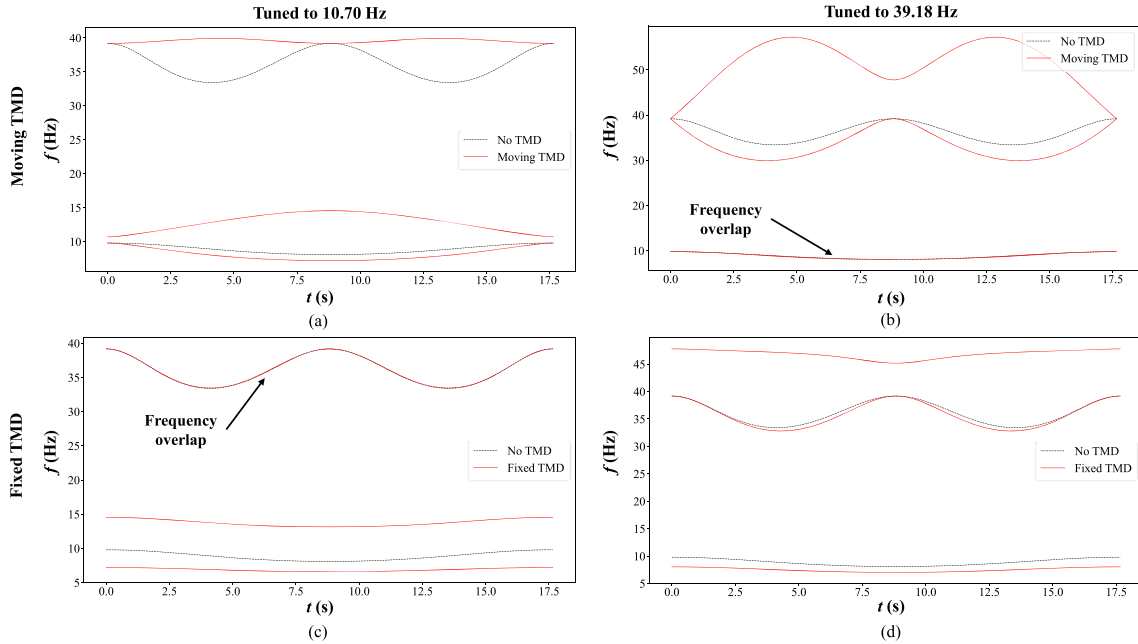
$$-\mathbf{A}_n^{-1}(n\Delta t)\mathbf{B}_n(n\Delta t) \tag{9}$$

5 Numerical study

The numerical example studied here is based on a mathematical model developed for simulating an experiment involving a heavy mass traversing a simply supported HEB 100 steel beam conducted by the authors [15], see Fig. 1. The relevant numerical values for the mechanical properties of the primary-secondary structural system configurations are listed in Tables 2 and 3. It is noted that damping in the TMD is provided by the spring element alone, as there is no dedicated damper. Thus, the amount of damping is truly minimal, thus leading to a sub-optimal TMD design. In terms of the analysis, minimal damping allows for a clear picture of the evolution of the eigenfunctions of the combined structural system with passage time of the heavy mass, as shown in Fig. 2. As previously mentioned, the presence of the TMD adds an extra degree-of-freedom to supplement the two generalized coordinates used to model the supporting continuous beam. Note that the TMD, as a separate SDOF structural system, has its own eigenfrequency, which can be designed to coincide with one of the eigenfrequencies of the simply supported beam. This is done by simply changing the stiffness parameter

Table 2 Mechanical properties for the simply supported HEB 100 steel section

ρ (tn/m^3)	A (m^2)	E (GPa)	I (m^4)	ξ_1	ξ_2	ρAL (tn)	L (m)	f_1 (Hz)	f_2 (Hz)
7.65	$26 \cdot 10^{-4}$	198.5	$450 \cdot 10^{-8}$	0.0021	0.0084	0.116	5.83	9.80	39.18

**Fig. 2** Eigenfrequency f_i (Hz) evolution with the passing of the heavy mass in the presence of a TMD moving with that mass (top row) and fixed at mid-span (bottom row): TMD tuning is with respect to **a, c** the first mode and **b, d** the second mode**Table 3** The moving mass and the TMD properties

M (tn)	v (m/s)	Fixed location L_1 (m)	TMD mass m (tn)	TMD stiffness k (kN/m)	TMD damping ξ	f (Hz)
0.027	0.33	2.915	0.027	122.0/1637.0	0.0075	10.70/39.18

k , hence the two different values listed in Table 3. In this case, it modifies the corresponding eigenfunction, leaving the remaining ones unchanged. In our case however, since the fixed TMD is placed at center span which is a nodal point for the second eigenfunction, the corresponding eigenfunction remains virtually unaffected. The evolution of the eigenfrequencies of the original primary system is also shown for comparison purposes.

More specifically, for both TMD configurations, the spring component's stiffness k is chosen so that this secondary SDOF system configuration is tuned to either the first or the second eigenfrequency of the primary structure. All computations regarding the eigenanalysis of the fundamental matrix of Eq. (9) are performed for each time step $\Delta t = 1/128$ s using the QR-Householder algorithm and the resulting eigenvalues come as complex conjugate pairs. Solving for the characteristic polynomial of Eq. (9) was found to be an unstable computation, because small perturbations of the polynomial's coefficients results in large variations of its complex roots [16]. It is finally mentioned that both eigenfrequencies ω_i and generalized coordinates \mathbf{y}_n^T are used as initial conditions for the computation of the immediately next time step values ω_{i+1} and \mathbf{y}_{n+1}^T .

Results are also presented in the form of spectrograms [18] for the power spectral density (PSD) in dB/Hz of the primary system transient accelerations $\ddot{w}(x = 3L/4, t)$ and likewise for the relative TMD acceleration $\ddot{u}_r(t)$ in Figs. 3 and 4 for the moving and the fixed TMDs, respectively. This way, both their time evolution and frequency content becomes visible. In the construction of the spectrograms, a 256 point Hanning window was applied to the transient records with an overlap of 250 points. More specifically, for both TMD configurations,

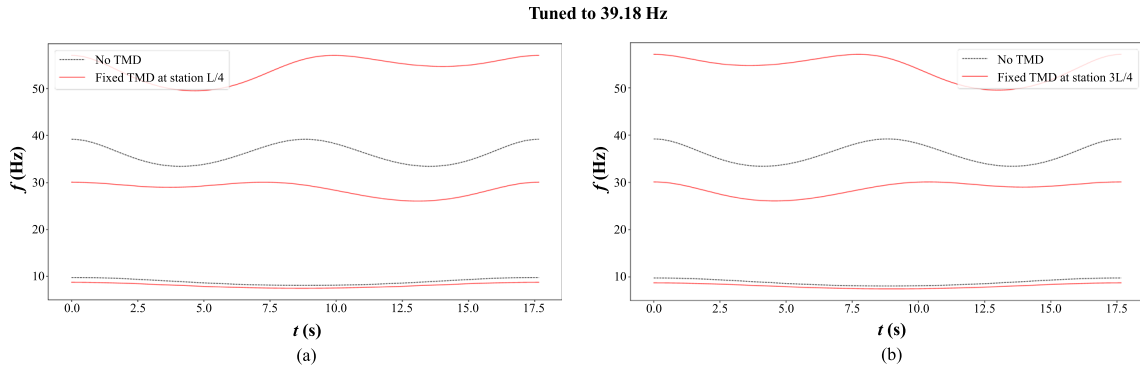


Fig. 3 Eigenfrequency f_i (Hz) evolution with the passing of the moving heavy mass in the presence of a TMD fixed at two stations on the beam: **a** $x = L/4$ and **b** $x = 3L/4$. Note that TMD tuning is with respect to the second mode

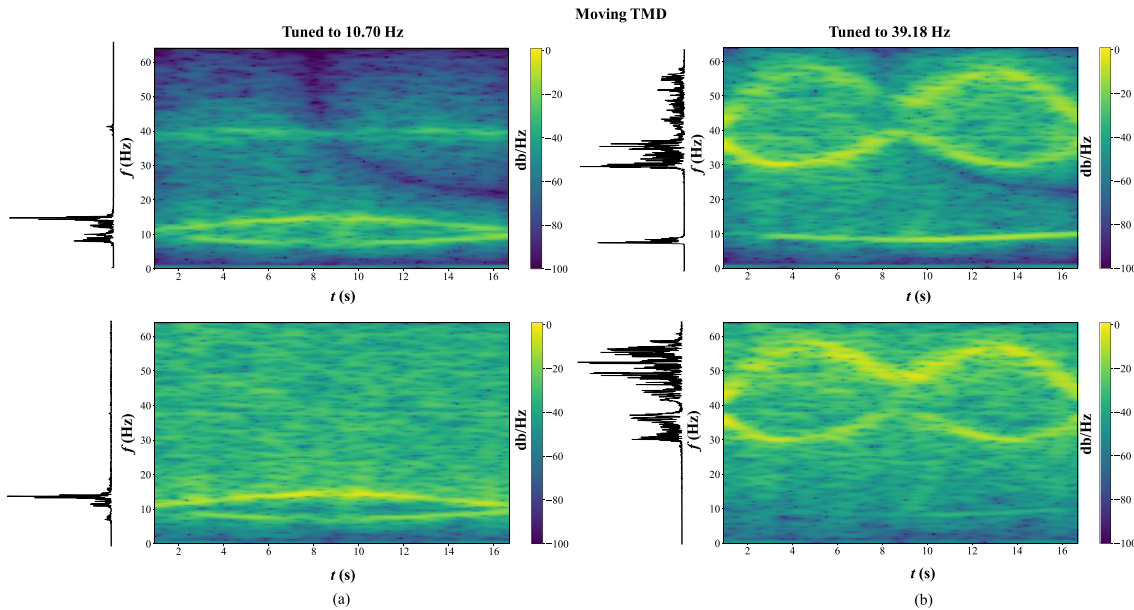


Fig. 4 Spectrograms for the moving TMD with the transient accelerations computed at station $x = 3L/4$ (top row) and the relative TMD acceleration \ddot{u}_r (bottom row). The TMD tuning is with respect to **a** the first mode and **b** the second mode of the primary structure

the spring component's stiffness k is chosen so that this secondary SDOF system configuration is tuned to either the first or the second eigenfrequency of the primary structure.

Obviously, the behavior of the traveling vehicle as a separate system can be studied either from the time series recorded by sensors placed directly on the bridges, or from sensors located in the moving vehicles [19]. If certain frequency bands of interest are not detected in the time series recorded by the sensors, (e.g., areas marked by a light-yellow color instead of deep yellow in the spectrograms of Fig. 4), their energy level can be enhanced by using adaptive amplifiers mounted on the moving vehicles. This subject is discussed in detail in some recent publications [20, 21].

Examining at first the response of the TMD itself, we observe that it is more predictable for the fixed case, in the sense that most vibratory energy is concentrated around its own fundamental frequency. This is especially true for tuning with respect to the low (first) eigenfrequency of the primary structure. When tuning is with respect to the second eigenfrequency, vibratory energy is more diffused. This behavior is more pronounced for the case of the moving TMD as opposed to the fixed TMD, meaning that the former vibrates over a wider range of frequencies, thus avoiding resonance (Fig. 5).

However, since of interest is the response of the primary system, and for the fixed TMD case, we observe that it operates successfully when tuned to the first eigenfrequency, as it absorbs most of the vibratory energy

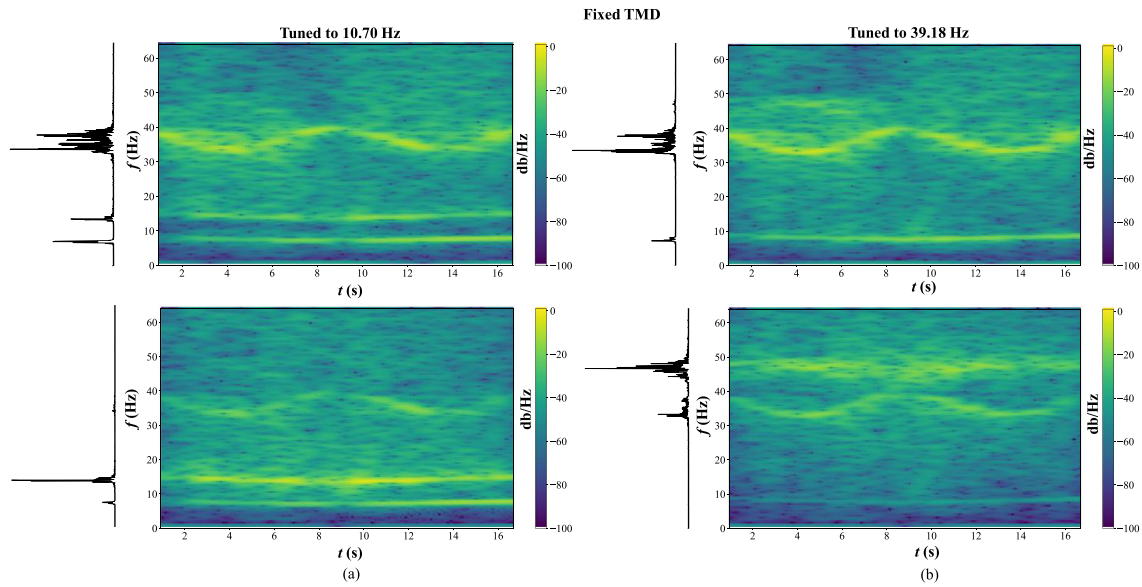


Fig. 5 Spectrograms for the fixed TMD with the transient accelerations computed at station $x = 3L/4$ (top row) and the relative TMD acceleration \ddot{u}_r (bottom row). The TMD tuning is with respect to **a** the first mode and **b** the second mode of the primary structure

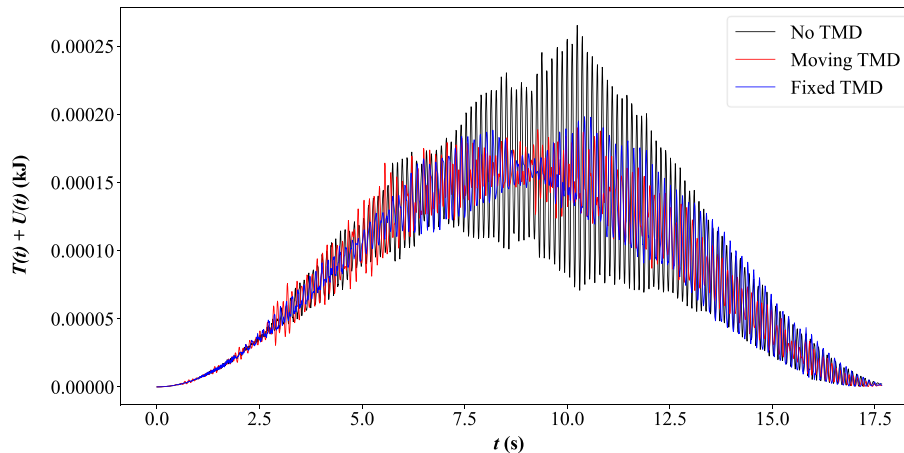


Fig. 6 Potential and kinetic energy development in the beam during the passage time of the heavy mass in the absence of a TMD, and in the presence of a moving TMD and a fixed TMD at $x = L/2$. Both TMD's are tuned to the first eigenfrequency of $f_1 = 10.70$ Hz

from that frequency range. However, when tuning is with respect to the second eigenfrequency, effectiveness is diminished as the primary system vibrates in bands around both the first and the second eigenfrequency. The effect of the moving TMD on the primary system is different, because irrespective of tuning, vibrations are primarily in the low frequency range around its first eigenfrequency, which is exactly the area that should be avoided. One positive fact about the moving TMD, however, is that does suppress the higher frequency vibrations when tuned to the lower frequency (Fig. 6).

In closing, the sum of the kinetic and potential energy in the beam as the heavy mass moves along its upper flange is expressed in terms of the first two generalized coordinate as follows:

$$T(\dot{q}_1, \dot{q}_2) = \frac{1}{2}(\dot{q}_1^2(t) + \dot{q}_2^2(t)), \quad U(q_1, q_2) = \frac{1}{2}(\omega_1^2 q_1^2(t) + \omega_2^2 q_2^2(t)) \quad (10)$$

6 Discussion and conclusions

This study focuses on the difference in passive vibration protection offered by a simple TMD (acting as a secondary SDOF system) when placed at a fixed point on the bridge (the primary system) versus the suspension system associated with a vehicle modeled as a heavy traveling mass that is the source of vibration. At first, it should be noted that the TMD parameters (mass, stiffness, damping) can be chosen so that its eigenfrequency coincides with one of the eigenfrequencies of the primary system, leading to what is known as optimal tuning. Of course, this optimization process depends heavily on the frequency content of the excitation. A further variable is the question of placement of the fixed TMD on the primary structure, which is usually approached in an ad hoc way, meaning that for simple cases such as the simply supported beam, placement is around mid-span. For the specific problem at hand, additional variables are the speed of traverse and the magnitude of the moving mass.

The time-dependence of the eigenproperties of a structure alludes to a non-autonomous mathematical problem, resulting in a time-stepping eigenproblem solution that is computationally involved and possibly unstable, as updated initial conditions must be defined at the onset of every time step of the solution procedure.

From this brief parametric study, a predictable conclusion is that the fixed TMD operates locally and effectively absorbs vibrations in the frequency range for which it was design. It should be noted that the particular TMD studied lacked a damper and the low level of structural damping available derived from the metallic spring element. Because of this, there was leakage of vibratory energy back to the frequency range where it was supposed to be zero. This was even more pronounced for the moving TMD, which seems to simply ameliorate the vibrations radiating from the moving mass, hence the diffusion of the frequency bands of vibration observed around the first two eigenfrequencies of the beam.

Acknowledgements Results presented in this work have been produced using the Aristotle University of Thessaloniki High-Performance Computing Infrastructure. The first author (G.I.D.) acknowledges the Hellenic Foundation for Research and Innovation (HFRI) for a Ph.D. Fellowship under the third call for Ph.D. fellowships (Fellowship Number: 6522). The second author (G.D.M.) acknowledges a Mercator fellowship made available by the German Research Foundation (DFG) project SM 281/20-1 entitled 'Resilient Infrastructure Based on Cognitive Buildings', Professor Kay Smarsly, coordinator, Technical University of Hamburg, Germany.

Funding This work was supported by Hellenic Foundation for Research and Innovation grant number (6522) and Deutsche Forschungsgemeinschaft grant number (SM 281/20-1).

Data availability The data supporting the findings of this study are available within the article.

Declarations

Conflict of interest Both authors state that there is no conflict of interest.

References

1. Den Hartog, J.P.: Mechanical vibrations, 3rd edn. McGraw-Hill, New York (1947)
2. Soong, T.T., Dargush, G.F.: Passive energy dissipation systems in civil engineering. Wiley, Chichester, UK (1997)
3. Warburton, G.B.: Optimum absorber parameters for various combinations of response and excitation parameters. *Earthq. Eng. Struct. Dyn.* **10**, 381–401 (1982)
4. Peeters, B., De Roeck, G.: One-year monitoring of the Z24-Bridge: environmental effects versus damage events. *Earthq. Eng. Struct. Dyn.* **30**, 149–171 (2001)
5. Green, M.F., Cebon, D., Cole, D.J.: Effects of vehicle suspension design on the dynamics of highway bridges. *J. Struct. Eng. ASCE* **121**(2), 272–282 (1995)
6. Cantero, D., Hester, D., Brownjohn, J.: Evolution of bridge frequencies and modes of vibration during truck passage. *Eng. Struct.* **152**, 452–464 (2017)
7. Etefagh, M.M., Behkamkia, D., Pedrammehr, S., Asadi, K.: Reliability analysis of the bridge dynamic response in a stochastic vehicle-bridge interaction. *KSCE J. Civ. Eng.* **19**(1), 220–232 (2015). <https://doi.org/10.1007/s12205-013-0388-8>
8. Yang, Y.B., Cheng, M.C., Chang, K.C.: Frequency variation in vehicle bridge interaction systems. *Int. J. Struct. Stab. Dyn.* **13**(2), 1350019 (2013)
9. Jin, S., Tan, C.A., Lu, H.: Vehicle suspension tuning for bridge-friendliness and influence on coupled vehicle-bridge system frequency. *Eng. Struct.* **304**, 117649 (2024)
10. Cantero, D., McGetrick, P., Kim, C.W., O' Brian, E.: Experimental monitoring of bridge frequency evolution during the passage of vehicles with different suspension properties. *Eng. Struct.* **187**, 209–219 (2019)

11. Yang, Y.B., Li, Z., Wang, Z.L., Shi, K., Xu, H., Qiu, F.Q., Zhu, J.F.: A novel frequency-free movable test vehicle for retrieving modal parameters of bridges: theory and experiment. *Mech. Syst. Signal Process.* **170**, 108854 (2022)
12. Lee, J., Lee, J., Kim, R.E.: Spatio-temporal frequency evaluation of a railroad bridge considering vehicle-bridge interaction. In: proceedings, experimental vibration analysis for civil engineering (EVACES 2023), M. P. Limongelli et al. (eds.), p. 721–730 (2023). https://doi.org/10.1007/978-3-031-39117-0_74
13. Mostafa, N., Di Maio, D., Loendersloot, R., Tinga, T.: The influence of vehicle dynamics on the time-dependent resonances of a bridge. *Adv. Bridge Eng.* **4**, 22 (2023). <https://doi.org/10.1186/s43251-023-00102-4>
14. Homaei, H., Dimitrakopoulos, E.G., Bakhshi, A.: Vehicle-bridge interaction and the tuned-mass damper effect on bridges during vertical earthquake excitation. *Acta Mech.* (2023). <https://doi.org/10.1007/s00707-023-03533-2>
15. Manolis, G.D., Dadoulis, G.I.: Passive control in a continuous beam under a travelling heavy mass: dynamic response and experimental verification. *Sensors* **24**(2), 573 (2024)
16. Manolis, G.D., Dadoulis, G.I.: On the numerical treatment of the discontinuity arising from a time-varying point mass attachment on a waveguide. *Algorithms* **16**(1), 26 (2023). <https://doi.org/10.3390/a16010026>
17. Dadoulis, G.I., Manolis, G.D.: Dynamic response of a damaged bridge span traversed by a heavy point mass. *J. Sound Vib.* **551**, 117613 (2023)
18. Brandt, A.: *Noise and vibration analysis: signal analysis and experimental procedures*. Wiley, Chichester (2011)
19. Wang, Z.L., Yang, J.P., Shi, K., Xu, H., Qiu, F.Q., Yang, Y.B.: Recent advances in researches on vehicle scanning method for bridges. *Int. J. Struct. Stab. Dyn.* **22**(15), 2230005 (2022)
20. Yang, Y.B., Wang, Z.L., Shi, K., Hao, X., Yang, J.P.: Adaptive amplifier for a test vehicle moving over bridges: theoretical study. *Int. J. Struct. Stab. Dyn.* **21**(3), 2150042 (2021)
21. Xu, H., Yang, M., Yang, J.P., Wang, Z.L., Shi, K., Yang, Y.B.: (2023) Vehicle-scanning method for bridges enhanced by dual amplifiers. *Struct. Control. Health Monit.* **1**, 6906855 (2023)

Publisher's Note Springer Nature remains neutral with regard to jurisdictional claims in published maps and institutional affiliations.